Organic & Biomolecular Chemistry

Cite this: *Org. Biomol. Chem.*, 2012, **10**, 2218

www.rsc.org/obc

COMMUNICATION

Experimental electron density of sumanene, a bowl-shaped fullerene fragment; comparison with the related corannulene hydrocarbon†‡

Stefan Mebs,*[a,b] Manuela Weber,[a] Peter Luger,[a] Bernd M. Schmidt,[a] Hidehiro Sakurai,[c] Shuhei Higashibayashi,[c] Satoru Onogi[c] and Dieter Lentz*[a]

Received 6th December 2011, Accepted 16th January 2012
DOI: 10.1039/c2ob07040e

The experimental electron density of sumanene, $C_{21}H_{12}$, was extracted from a high resolution X-ray data set measured at 100 K and topologically analyzed. In addition to bond topological and atomic properties, information about the density distribution between adjacent molecules, which show close C···C approaches of ~3.4 Å within the columnar π-stacks in the crystal lattice, are discussed. A comparison is made with the electron density of the related corannulene molecule based also on the analysis of Electron Localizability Indicator (ELI-D) calculations.

Sumanene, $C_{21}H_{12}$, is a bowl-shaped π-conjugated carbon system, having a C_{3v}-symmetric structural motif present in fullerenes and carbon nanotubes. Compared to corannulene, $C_{20}H_{10}$, sumanene is characterized by three benzylic positions which allow further functionalization and deepen the molecular bowl (1.11 Å)[1] in comparison to the bowl-depth of corannulene (0.87 Å).[2] Both compounds possess significantly alternating bonds. They are relevant, not only as model compounds for fullerenes, but also because of their own chemical and physical properties. It is interesting to note that a detailed theoretical study on the sumanene structure had appeared in 2001[3] even before the molecule could be synthesized in 2003.[4]

Its crystal structure was elucidated in 2005, showing 1D columnar π-stacking in a convex–concave fashion.[1] Close C···C contacts around 3.4 Å exist between adjacent molecules which are 60° displaced against each other along the stacking axis (Fig. 1, left). This columnar arrangement is in sharp contrast to the solid-state structure of corannulene, which is dominated by CH···π interactions and a packing without columnar order.[2] Usually, a columnar type of π-stacking is observed for larger systems, like hemifullerene,[8] indenocorannulenes[9] or as a result of attractive interactions with metal-complexes[10] or metal-surfaces.[11]

These types of noncovalent interactions are central to many areas of supramolecular[12] chemistry and are traditionally explained by π-polarization effects,[13] or recently by a local, direct interaction model.[14] This is not only of theoretical interest, because many organic materials are successfully used in molecular electronics.[15] Anisotropic electron-transport properties were investigated for the needle-like crystals of sumanene and showed high electron mobility examined by time-resolved microwave conductivity methods. These results suggest a noticeable HOMO–LUMO overlap between the adjacent bowls.[16]

[a]*Freie Universität Berlin, Institut für Chemie und Biochemie – Anorganische Chemie, Fabeckstr. 34-36 und Fabeckstr. 36a, 14195 Berlin, Germany. E-mail: lentz@chemie.fu-berlin.de; Fax: +49 030 83853464; Tel: +49 030 83852695*
[b]*Humboldt Universität Berlin, Mathematisch-Naturwissenschaftliche Fakultät I, Institut für Chemie, Anorganische und Allgemeine Chemie I, Brook-Taylor-Str. 2, 12489 Berlin, Germany*
[c]*Research Center for Molecular Scale Nanoscience, Institute for Molecular Science, Myodaiji, Okazaki 444-8787, Japan*

†Electronic supplementary information (ESI) available: Fig. of ELI-D representations and deformation density of sumanene, tables of bond topological, atomic and ELI-D properties. An extended discussion involving a thorough analysis of N(ELI) data in comparison to different C–C bonds and B–B bonds is presented. CCDC 831828. For ESI and crystallographic data in CIF or other electronic format see DOI: 10.1039/c2ob07040e

‡Crystallographic data: $C_{21}H_{12}$, rhombohedral, R3c, a = 16.575(1), c = 7.580(1), V = 1803.5 Å^3, Z = 6, T = 100 K. Data collection on a Bruker 1 K diffractometer (MoKα radiation, graphite monochromator, λ = 0.71068 Å), N_2 gas stream cooling. Total no. of reflections 81 481, unique 7175 (6459 with $I > 3\sigma$), R_{int} = 0.035, multipole refinement with XD[25] up to hexadecapoles. $R(F)/R_{all}(F)/R_w(F)$ = 0.022/0.031/0.023, Gof = 1.18, N_{ref}/N_v = 41.67, max/min res. dens. ≤|0.27| eÅ^{-3}.

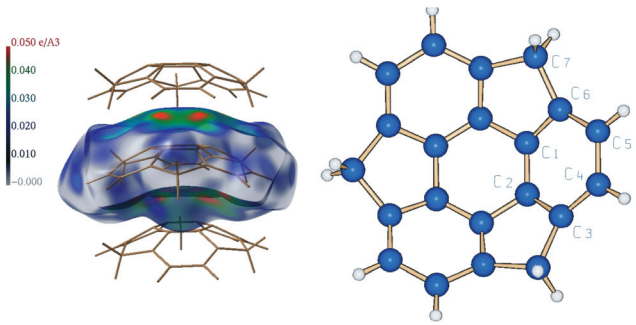

Fig. 1 Left: Arrangement of adjacent molecules of $C_{21}H_{12}$ in columnar π-stacks as a Hirshfeld surface representation.[5] Deeply colored sections represent regions with close intermolecular contacts less than 3.5 Å. Right: Molecular structure of $C_{21}H_{12}$ showing also the atomic numbering scheme in the asymmetric unit, and the notation of bond-types: C1–C2 = h = hub, C1–C6 = s = spoke, C3–C4 = f = flank, C4–C5 = r = rim.[6,7]

Table 1 C···C contacts less than 3.5 Å

Contact[a]	Sym. for atom 2	d (Å)	Bond path (Å)	$\rho(\mathbf{r}_b)$ (eÅ^{-3})	$\nabla^2\rho(\mathbf{r}_b)$ (eÅ^{-5})
C1(H)···C5(R6) 0.019 − 0.394	$1-y,1-x,1/2+z$	3.375	—	—	—
C1(H) ··· C6(S) 0.019 − 0.060	$1-y,1-x,1/2+z$	3.418	3.451	0.05	0.44
C2(H) ··· C3(S) 0.019 − 0.060	$x,2+x-y,1/2+z$	3.404	3.451	0.05	0.42
C2(H) ···C4(R6) 0.019 − 0.394	$x,2+x-y,1/2+z$	3.446	—	—	—
C6(S) ···C5(R6) −0.060 −0.394	$1-y,1-x,1/2+z$	3.417	3.423	0.04	0.38

[a] In parentheses: atom types (H = hub, S = spoke, R5, R6 = rim), second line: atomic charge.

Consequently it is valuable to investigate the electron density (ED) of sumanene and to analyze the ED distribution in the intermolecular regions with close C···C contacts. The ED of the related corannulene molecule is selected for comparison.[17]

From a high resolution X-ray data set [$(\sin\theta/\lambda)_{max}$ = 1.30 Å^{-1}] of 81 481 reflections, measured at 100 K, an experimental electron density distribution was obtained by application of the Hansen & Coppens multipole formalism.[18] A topological analysis, according to Bader's QTAIM theory,[19] was carried out and yielded bond-topological and atomic properties summarized in the ESI (see Tables S1 and S2†). This study was complemented by an analysis of the Electron Localizability Indicator (ELI-D)[20] of the optimized gas-phase structure[21] not only for sumanene but also for corannulene for comparison. ELI-D divides space into regions of localized electron pairs instead of atoms and therefore greatly complements the AIM theory.

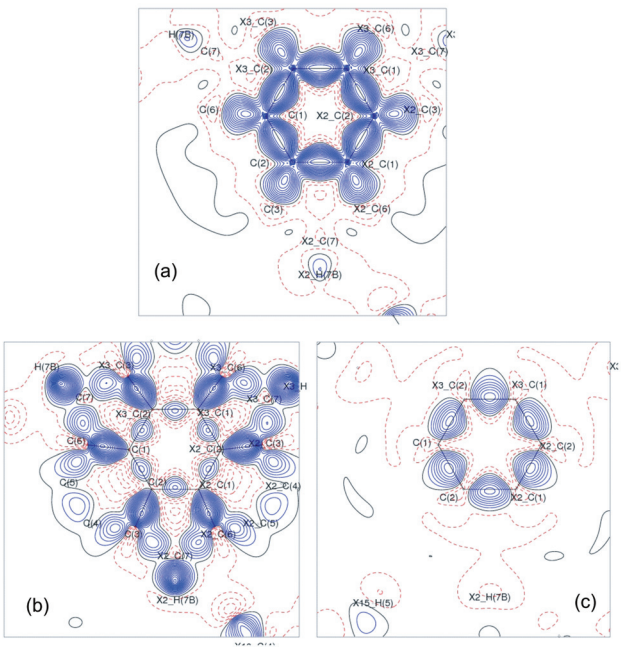

Fig. 2 Static deformation densities in the six-membered ring (a) and in parallel planes 0.4 Å towards the interior (b) and 0.4 Å towards the exterior (c) of the bowl. Contour intervals 0.05 eÅ^{-3}.

The molecular structure of sumanene is shown in Fig. 1 (right), giving also the atom numbering scheme of the molecular fragment in the asymmetric unit (one third of the molecule). In accordance with the notation chosen in the literature by Scott and co-workers (see for example ref. 6) for the bond-type names (see also legend of Fig. 1), we use a H = hub, S = spoke, and R = rim to differentiate atom types in the molecules.

Fig. 2 illustrates that some charge displacement has taken place towards the outer surface of the sumanene bowl. Static deformation densities were generated in the plane of the central six-membered ring (Fig. 2a) and in parallel planes 0.4 Å towards the interior (Fig. 2b) and the exterior (Fig. 2c) of the bowl, respectively. Comparison of Fig. 2b and 2c shows that higher density is found in the exterior plane.

This effect was also found in the corannulene molecule, but the difference between the exterior and interior ring density is about a factor of two higher in the present case which seems to be related to the greater depth of the sumanene bowl compared to that of corannulene.[1,2]

As mentioned earlier, there are close C···C contacts between directly adjacent molecules of the column. Five contacts of this type exist with distances between 3.38 and 3.45 Å (Table 1). In three of these, bond critical points ($\mathbf{r}_b$) were located with electron densities of 0.04–0.05 eÅ^{-3}. Similar densities were found for contacts of 3.3 Å between hexagons of adjacent molecules in the crystal of the fullerene derivative $C_{60}(CF_3)_{12}$.[22]

The intermolecular electron density concentration is also visible on the Hirshfeld surface[23,24] in Fig. 1 (left). Although the contact distances in the above-mentioned fullerene and in the title compound are similar, the density distributions are different. There is a rather extended continuous torus-type density region in the fullerene, while in sumanene discrete density concentrations are seen between the C···C contacts. Fig. 3(a,b) depicts the experimental electrostatic potential (ESP) of the title molecule mapped on the iso-surface of the electron density at a value of 0.001 au (0.0067 eÅ^{-3}). The potential gradient, expressed by the max/min values (0.346/−0.183 eÅ^{-1}, see color bar), is greater than in corannulene (max/min 0.108/−0.089 eÅ^{-1}) in accordance with the higher atomic charge separation.

This is also supported by the results of a quantitative analysis of the ESP on the given ED iso-surface according to Politzer *et al.*[27] The positive and negative average potential values V_s^+ and V_s^- were calculated as given in ref. 28. V_s^+ and $|V_s^-|$ of

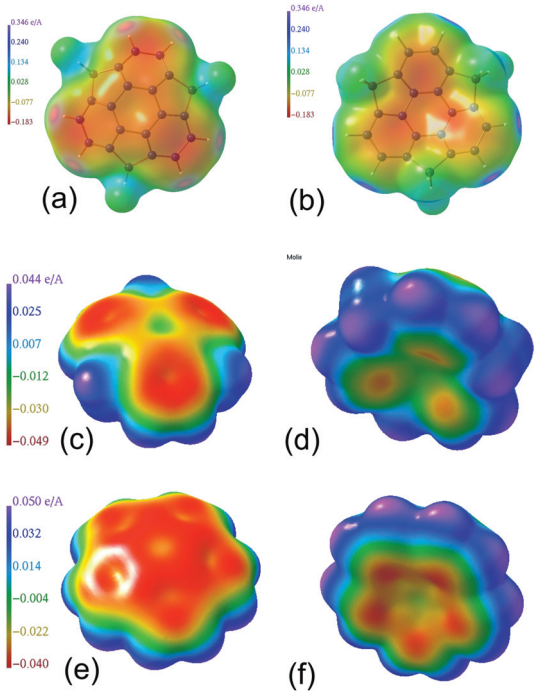

Fig. 3 (a) Electrostatic potential (ESP) of sumanene calculated from the experimental electron density[25,26] and mapped onto the iso-electron-density surface ρ = 0.001 au, exterior region. The color code is shown by the color bar; (b) same as (a), interior region; (c,d) corresponding ESPs from theoretical calculations on the isolated sumanene molecule; (e,f) ESPs from theoretical calculations on the isolated corannulene molecule.

0.074/0.091 eÅ^{-1} are larger for the title compound than for corannulene (0.046/0.034 eÅ^{-1}) indicating a stronger polarization in the sumanene bowl. The experimental ESPs (Fig. 3a,b) on the exterior and interior surface of the sumanene bowl show already an interchange of positive and negative potential in 60° sectors with respect to an axis perpendicular to the major molecular plane. This is even more pronounced for the potential derived from a theoretical calculation of the isolated molecule (Fig. 3c, d). We can conclude that this is – except for a certain smearing in the experimental case – already a molecular property. In contrast, for the theoretical potential of corannulene (Fig. 3e,f), an almost continuous negative region is seen on both surfaces.

Hence the ESP of sumanene allows a columnar stacking where positive and negative regions closely interact when adjacent molecules are rotated by 60° to each other. Evidences concerning the packing behavior are complemented by an ELI-D[20] interpretation of the bowl-to-bowl interactions within the crystal.

Fig. 4 and 5 give representations of the ELI-D for the optimized gas-phase structures of corannulene (Fig. 4a) and sumanene (Fig. 4b),[21] together with a calculated packing scheme of sumanene at two different ELI-D iso-values (Fig. 5a,b). The color code refers to the volumes of the electron-pair basins; green basins are smaller than blue basins. The five-fold symmetry in corannulene and the three-fold symmetry in sumanene are visible. Obviously, C–C bonding basins of five-membered rings are smaller and less populated than those of six-membered rings [N(ELI) (corannulene) r > s > f > h; (sumanene) f6 > r > h66 > s > h65 > f5].

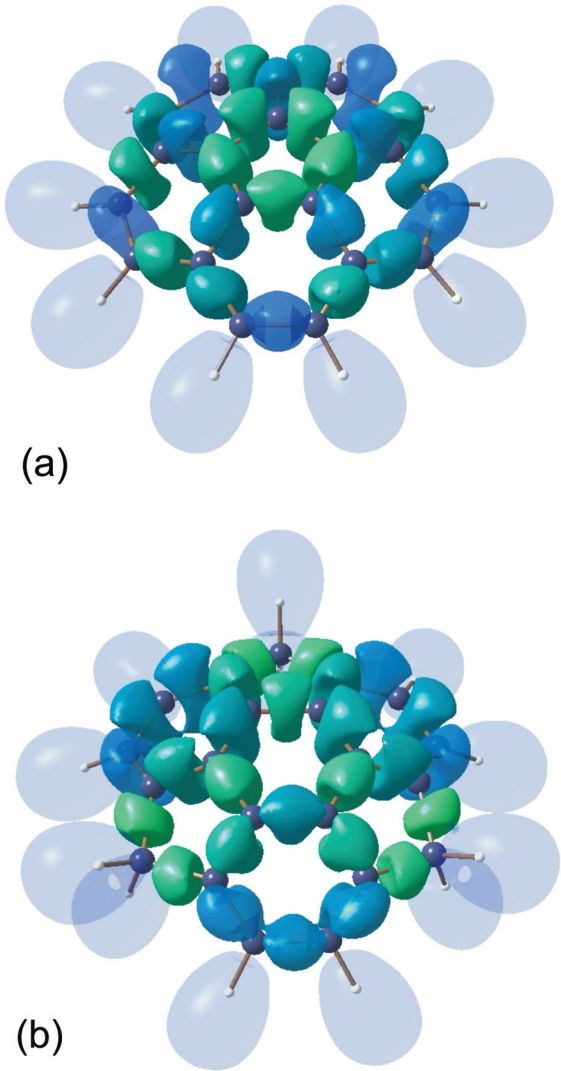

Fig. 4 (a), (b) Color-coded ELI-D representations of corannulene and sumanene in the gas phase at an iso-value of γ = 1.25.

The ED derived data such as $\rho(\mathbf{r}_{bcp})$, the integrated amount of ED within the C–C zero flux surface (zfs), and the kinetic and total energy density over ρ ratios (G/ρ, H/ρ) show linear relations with respect to the bond distance (Fig. 6a).

This can even be extended to a large number of compounds including C_{60} and C_{70}[29] (Fig. S5†). Deviations are observed for the halogen substituted bonds of $C_{60}Cl_{30}$ and $C_{60}F_{18}$,[30] respectively. A similar linear relationship can be observed for some recently published borane cage compounds,[31] whereas the charge density at the ring critical points exhibits an exponential behavior (Fig. S5†) with respect to bond length.

However, data reflecting the pair density, like the delocalization index (δ(C,C)) and the electron population of the C–C bonding basins (N(ELI)), provide a more detailed view, see Fig. 6b. The general trend of decreasing electron populations (in terms of δ(C,C) and N(ELI)) in the C–C bonds with increasing bond distances is basically retained. Thus, the ELI-D supports the dominant presence of mesomeric forms as given in Fig. 7 (see data in Table S3†).

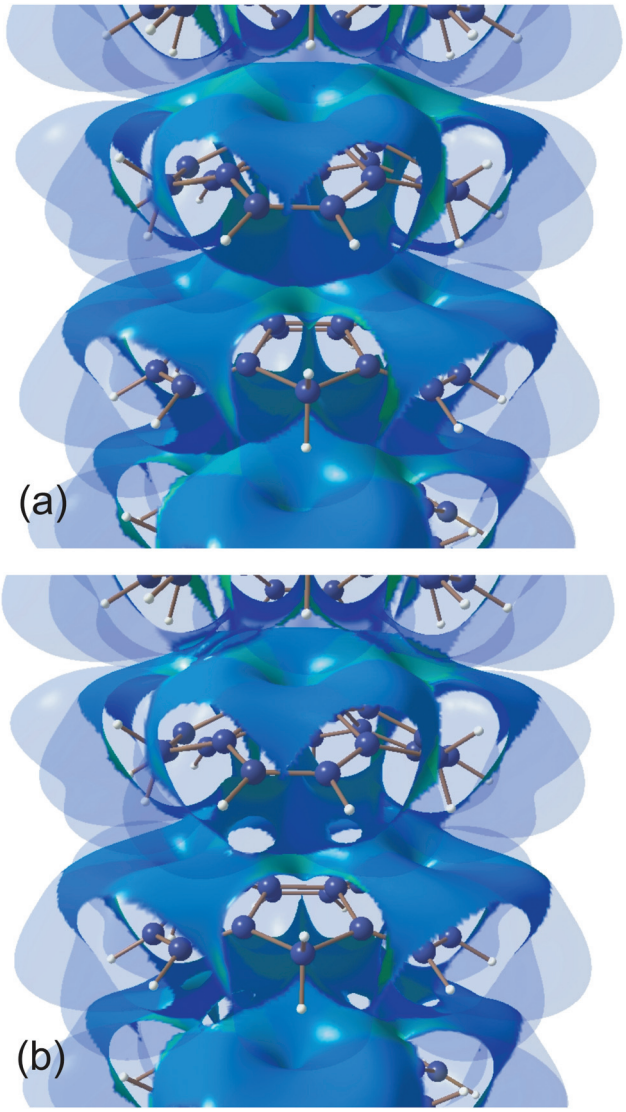

Fig. 5 (a), (b) ELI-D representations of a sumanene packing scheme including five sumanene molecules. $\gamma = 0.60$ (a) and $\gamma = 0.55$ (b).

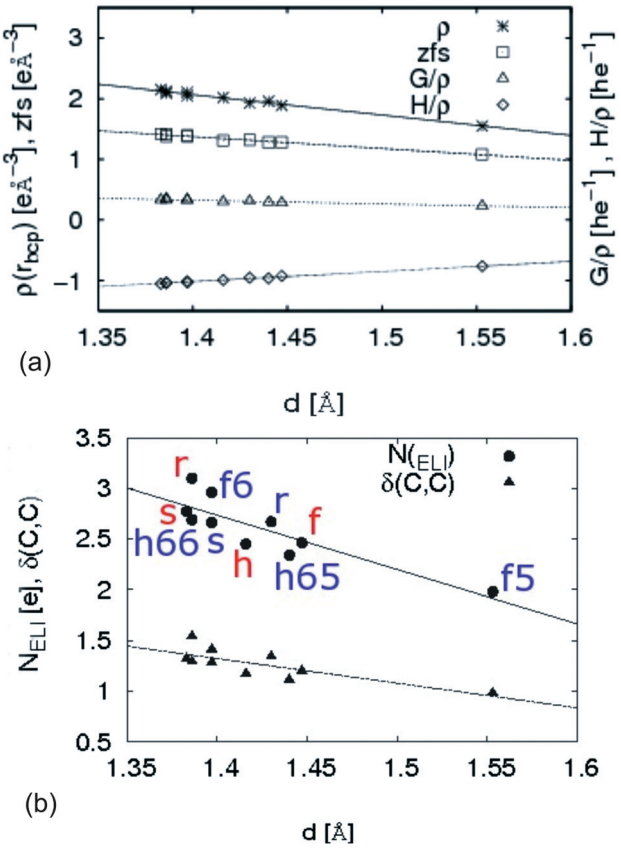

Fig. 6 (a) Theoretically calculated ED-properties plotted against the C–C bond distances in corannulene and sumanene. (b) Corresponding properties for electron localization plotted against the C–C bond distances. Red labels refer to corannulene, blue labels refer to sumanene.

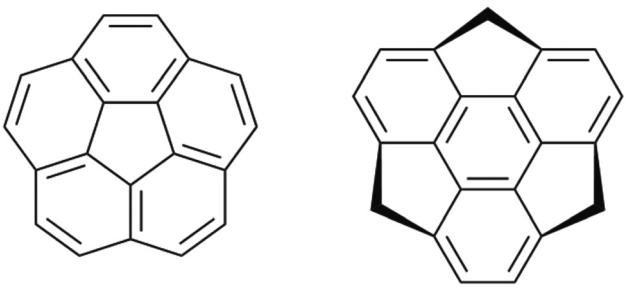

Fig. 7 Dominant mesomeric forms for free corannulene (left) and sumanene (right).

In addition, inspection of Fig. 6b reveals that "flank" and "rim" bonds in relation to the bond distances are generally characterized by larger N(ELI)-values in comparison to "hub" and "spoke" bonds. The considerable accumulation of electrons at the outer regions of the corannulene molecule also might influence the packing scheme in the crystal. The results are supported by the saddle-point analysis of the ELI-D field which shows a separation of rim and flank bonds from hub and spoke bonds, see Fig. S3 and S4 of the ESI† for more details.

For the analysis of intermolecular interactions the ELI-D is a useful extension to bond topology, electrostatic potential, and Hirshfeld surface. If the ELI-D iso-surface is stepwise decreased, one primarily finds all electron pair basins within one molecule to be merged as displayed in Fig. 5a ($\gamma = 0.60$; for clarity the protonated basins are shown in transparent mode). At this iso-value the molecules are totally separated from each other. A further decrease of the iso-value connects adjacent molecules (see Fig. 5b $\gamma = 0.55$) at defined regions, where intermolecular interactions take place. This is confirmed by the topological analysis of the ELI-field, which shows saddle-points at these sites, see illustration S1 in the ESI†. A closer view of Fig. 5b reveals that these contacts are between an f5-bond of one sumanene molecule and an f6-bond of another one. Interestingly, the central six-membered rings are still separated at this iso-value. Probably, the sterical demands of the hydrogen atoms connected to the five-membered rings prevent a closer contact between the central six-membered rings of two neighbored molecules. This is in accordance with the absence of corresponding bond critical points in the ED as well as in the ELI-D.

In summary, we have shown that sumanene is indeed more strongly polarized than corannulene, which may introduce the

columnar arrangement in the solid state by attractive interaction between the π-acidic five-membered ring and the electron-rich six-membered rings, according to the ESP. The increased strain in the sumanene bowl is accompanied by a pronounced shift of electron density to the exterior surface of the bowl. We found a simple relationship between C–C distances and the electron-pair basins, which can be valuable for the analysis of new carbon-rich compounds, without the need to obtain high-resolution X-ray data sets.

Acknowledgements

This work was funded by the Deutsche Forschungsgemeinschaft (DFG), grants Lu222/30-2 and Le423/13-3 within the special priority program SPP1178 and the Center of Supramolecular Interactions of the Freie Universität Berlin. H. S. thanks MEXT and JST-PRESTO for financial support. B. M. S. thanks the JSPS for a scholarship.

Notes and references

1 H. Sakurai, T. Daiko, H. Sakane, T. Amaya and T. Hirao, *J. Am. Chem. Soc.*, 2005, **127**, 11580–11581.
2 J. C. Hanson and C. E. Nordman, *Acta Crystallogr., Sect. B: Struct. Crystallogr. Cryst. Chem.*, 1976, **B32**, 1147–1153.
3 U. D. Priyakumar and G. N. Sastry, *J. Phys. Chem. A*, 2001, **105**, 4488–4494.
4 H. Sakurai, T. Daiko and T. Hirao, *Science*, 2003, **301**, 1878.
5 MOLISO: C. B. Hübschle and P. Luger, *J. Appl. Crystallogr.*, 2006, **39**, 901–904.
6 M. A. Petrukhina, K. W. Andreini, J. Mack and L. T. Scott, *J. Org. Chem.*, 2005, **70**, 5713–5716.
7 E. Keller and J. S. Pierrard, SCHAKAL99, Albert-Ludwigs University of Freiburg, Germany, 1999.
8 M. A. Petrukhina, K. W. Andreini, L. Peng and L. T. Scott, *Angew. Chem.*, 2004, **116**, 5593–5597.
9 (*a*) Y.-T. Wu, T. Hayama, K. K. Baldridge, A. Linden and J. S. Siegel, *J. Am. Chem. Soc.*, 2006, **128**, 6870–6884; (*b*) A. S. Filatov, L. T. Scott and M. A. Petrukhina, *Cryst. Growth Des.*, 2010, **10**, 4607–4621; (*c*) E. A. Jackson, B. D. Steinberg, M. Bancu, A. Wakamiya and L. T. Scott, *J. Am. Chem. Soc.*, 2007, **129**, 484–485.
10 (*a*) A. S. Filatov, E. A. Jackson, L. T. Scott and M. A. Petrukhina, *Angew. Chem., Int. Ed.*, 2009, **48**, 8473–8475; (*b*) A. S. Filatov, A. K. Green, E. A. Jackson, L. T. Scott and M. A. Petrukhina, *J. Organomet. Chem.*, 2011, **696**, 2877–2881.
11 T. Bauert, K. K. Baldridge, J. S. Siegel and K.-H. Ernst, *Chem. Commun.*, 2011, **47**, 7995–7997.
12 P. A. Denis, *Chem. Phys. Lett.*, 2011, **516**, 82–87.
13 F. Cozzi, M. Cinquini, R. Annunziata, T. Dwyer and J. S. Siegel, *J. Am. Chem. Soc.*, 1992, **114**, 5729–5733.
14 S. E. Wheeler, *J. Am. Chem. Soc.*, 2011, **133**, 10262–10274.
15 (*a*) S. Allard, M. Forster, B. Souharce, H. Thiem and U. Scherf, *Angew. Chem., Int. Ed.*, 2008, **47**, 4070–4098; (*b*) L. Zoppi, L. Martin-Samos and K. K. Baldridge, *J. Am. Chem. Soc.*, 2011, **133**, 14002–14009 and references therein.
16 T. Amaya, S. Seki, T. Moriuchi, K. Nakamoto, T. Nakata, H. Sakane, A. Saeki, S. Tagawa and T. Hirao, *J. Am. Chem. Soc.*, 2009, **131**, 408–409.
17 S. Grabowsky, M. Weber, Y.-S. Chen, D. Lentz, B. M. Schmidt, M. Hesse and P. Luger, *Z. Naturforsch.*, 2010, **65b**, 452–460.
18 N. K. Hansen and P. Coppens, *Acta Crystallogr., Sect. A: Cryst. Phys., Diffr., Theor. Gen. Crystallogr.*, 1978, **A34**, 909–921.
19 R. F. W. Bader, *Atoms in Molecules*, Clarendon Press, Oxford, 1st edn, 1990.
20 M. Kohout, *Int. J. Quantum Chem.*, 2004, **97**, 651–658.
21 M. J. Frisch *et al.*, *Gaussian 98, revision a.7*, Gaussian, Inc., Pittsburgh PA, 1998.
22 L. Chęcińska, S. I. Troyanov, S. Mebs, C. B. Hübschle and P. Luger, *Chem. Commun.*, 2007, 4003–4005.
23 J. J. McKinnon, A. S. Mitchel and M. A. Spackman, *Chem.–Eur. J.*, 1998, **4**, 2136–2141.
24 M. A. Spackman and P. G. Byrom, *Phys. Lett.*, 1997, **267**, 215–220.
25 A. Volkov, P. Macchi, L. J. Farrugia, C. Gatti, P. R. Mallinson, T. Richter and T. Koritsanszky, Xd2006 – a computer program for multipole refinement, topological analysis and evaluation of intermolecular energies from experimental and theoretical structure factors, University at Buffalo, NY, (USA); University of Milano, (Italy); University of Glasgow, (UK); CNRISTM, Milano, (Italy); Middle Tennessee State University, TN, (USA), 2006.
26 A. Volkov, H. F. King, P. Coppens and L. J. Farrugia, *Acta Crystallogr., Sect. A: Found. Crystallogr.*, 2006, **A62**, 400–408.
27 P. Politzer, J. S. Murray and Z. Preralta-Inga, *Int. J. Quantum Chem.*, 2001, **85**, 676–684.
28 C. B. Hübschle, B. Dittrich, S. Grabowsky, M. Messerschmidt and P. Luger, *Acta Crystallogr., Sect. B: Struct. Sci.*, 2008, **B64**, 363–374.
29 R. Kalinowski, M. Weber, S. I. Troyanov, C. Paulmann and P. Luger, *Z. Naturforsch.*, 2010, **65b**, 1–7.
30 C. B. Hübschle, St. Scheins, M. Weber, P. Luger, A. Wagner, T. Koritsanszky and S. I. Troyanov, *Chem.–Eur. J.*, 2007, **13**, 1910–1920.
31 S. Mebs, R. Kalinowski, S. Grabowsky, D. Förster, R. Kickbusch, E. Justus, W. Morgenroth, C. Paulmann, P. Luger, D. Gabel and D. Lentz, *Inorg. Chem.*, 2011, **50**, 90–103.

